PRE-PROCESSING OF NEURO IMAGES CAPTURED THROUGH HIGH RESOLUTION OPTICAL MICROSCOPE USING 3D NEIGHBOURHOOD ANALYSIS

A thesis

Submitted in partial fulfilment of the requirement for the Degree of

Master of Technology in Computer Technology

Of

Jadavpur University

By

Suchandra Bose

Registration No.: 137114 of 2016-2017

Examination Roll No.: M6TCT19017

Under the Guidance of

Prof. Subhadip Basu

Department of Computer Science and Engineering

Jadavpur University, Kolkata-700032

India

2019

FACULTY OF ENGINEERING AND TECHNOLOGY

JADAVPUR UNIVERSITY

Certificate of Recommendation

This is to certify that the dissertation entitled "Pre-processing of Neuro Images captured through High Resolution Optical Microscope using 3D Neighbourhood Analysis" has been carried out by Suchandra Bose (University Registration No.: 137114 of 2016-17, Examination Roll No.:M6TCT19017) under my guidance and supervision and be accepted in partial fulfilment of the requirement for the Degree of Master of Technology in Computer Technology. The research results presented in the thesis have not been included in any other paper submitted for the award of any degree in any other University or Institute.

……

Prof. Subhadip Basu (Thesis Supervisor)
Department of Computer Science and Engineering
Jadavpur University, Kolkata-32

Countersigned

…….

Prof. Mahantapas Kundu
Head, Department of Computer Science and Engineering,
Jadavpur University, Kolkata-32.

…….

Prof. Chiranjib Bhattacharjee
Dean, Faculty of Engineering and Technology,
Jadavpur University, Kolkata-32.

FACULTY OF ENGINEERING AND TECHNOLOGY

JADAVPUR UNIVERSITY

Certificate of Approval*

This is to certify that the thesis entitled "Pre-processing of Neuro Images captured through High Resolution Optical Microscope using 3D Neighbourhood Analysis" is a bona-fide record of work carried out by Suchandra Bose in partial fulfilment of the requirements for the award of the degree of Master of Technology in Computer technology, in Department of Computer Science and engineering, Jadavpur University during the period of July 2016 to June 2019. It is understood that by this approval the undersigned do not necessarily endorse or approve any statement made, opinion expressed or conclusion drawn therein but approve the thesis only for the purpose for which it has been submitted.

……..

Signature of Examiner 1

Date:

……..

Signature of Examiner 2

Date:

*Only in case the thesis is approved

FACULTY OF ENGINEERING AND TECHNOLOGY

JADAVPUR UNIVERSITY

Declaration of Originality and Compliance of Academic Ethics

I hereby declare that this thesis entitled "Pre-processing of Neuro Images captured through High Resolution Optical Microscope using 3D Neighbourhood Analysis" contains literature survey and original research work by the undersigned candidate, as part of her Degree of Master of Technology in Computer Technology.

All information has been obtained and presented in accordance with academic rules and ethical conduct.

I also declare that, as required by these rules and conduct, I have fully cited and referenced all materials and results that are not original to this work.

Name: Suchandra Bose

Registration No: 137114 of 2016-2017

Exam Roll No.: M6TCT19017

Thesis Title: Pre-processing of Neuro Images captured through High Resolution Optical Microscope using 3D Neighbourhood Analysis

…..……..

Signature with Date

Acknowledgement

I would like to start by thanking the holy trinity for helping me deploy all the right resources and for shaping me into a better human being. I would like to express my deepest gratitude to my advisor**, Prof. Subhadip Basu**, Department of Computer Science and Engineering, Jadavpur University for his admirable guidance, care, patience and for providing me with an excellent atmosphere for doing research. Our numerous scientific discussions and his many constructive comments have greatly improved this work.

I would like to thank **Prof. Mita Nasipuri,** Co-ordinator of CMATER Lab, Department of Computer Science and Engineering, Jadavpur University for providing me all necessary infrastructure and facility to carry on this research.

I would like to thank **Prof. Mahantapas Kundu**, Head of the department, Department of Computer Science and Engineering, Jadavpur University for extending his help to complete this thesis.

I would like to thank **Dr. Andre Zeug**, Department of Cellular Neurophysiology, Center of Physiology, Hannover, Germany for providing me the problem statement and building the problem definition. I would like extend my gratitude to him for the provided confocal microscopic images upon which our proposed method works.

I would like to thank **Prof. Dr. Evgeni Ponimaskin**, Department of Cellular Neurophysiology, Center of Physiology, Hannover, Germany for providing me confocal microscopic images to test our algorithm. I extend my gratitude for his help and support.

I would like to thank **Dr. Jakub Wlodarczyk,** Department of Molecular and Cellular Neurobiology, Nencki Institute of Experimental Biology, Warsaw, Poland for providing the essential data for our research to test our method’s efficiency.

I am thankful to **Centre for Microprocessor Applications for Training Education** and Research for giving me the proper laboratory facility for carrying out my work.

I am deeply grateful to my senior Mr**. Nirmal Das** for his guidance and supervision throughout the project work. Without his enthusiasm, encouragement, support and continuous optimism this thesis would hardly have been continued. I would like to acknowledge his patience for teaching me about the Qt framework. I would like to thank him educating me about Mendeley, which has proved to be an indispensable tool to cite research papers and providing the template for this thesis.

Most importantly none of this would have been possible without the love and support of my family. I extend my thanks to my parents **Mr. Salil Kumar Bose** and **Mrs. Suchinta Bose**, parents-in-laws **Mr. Atanu Dutta** and **Mrs. Sarbani Dutta** whose forbearance and whole-hearted support helped this endeavour succeed. I am also thankful to my husband **Mr. Anirban Dutta** and my sister **Ms. Srestha Bose** who were always present to motivate me.

This thesis would not have been completed without the inspiration and support of a number of wonderful individuals — my thanks and appreciation to all of them for being part of this journey and making this thesis possible.

……..

Suchandra Bose
Registration No: 137114 OF 2016-17
Exam Roll No.: M6TCT19017
Department of Computer Science & Engineering
Jadavpur University

Contents

List of figures

Chapter 1

Introduction

1.1 Neurological image analysis: relevance to brain activity and neuro diseases

Neuroimaging or brain imaging[1] is a technique to depict the structure, function of the nervous system[2]. It is an important discipline within medicine, neuroscience, and psychology.

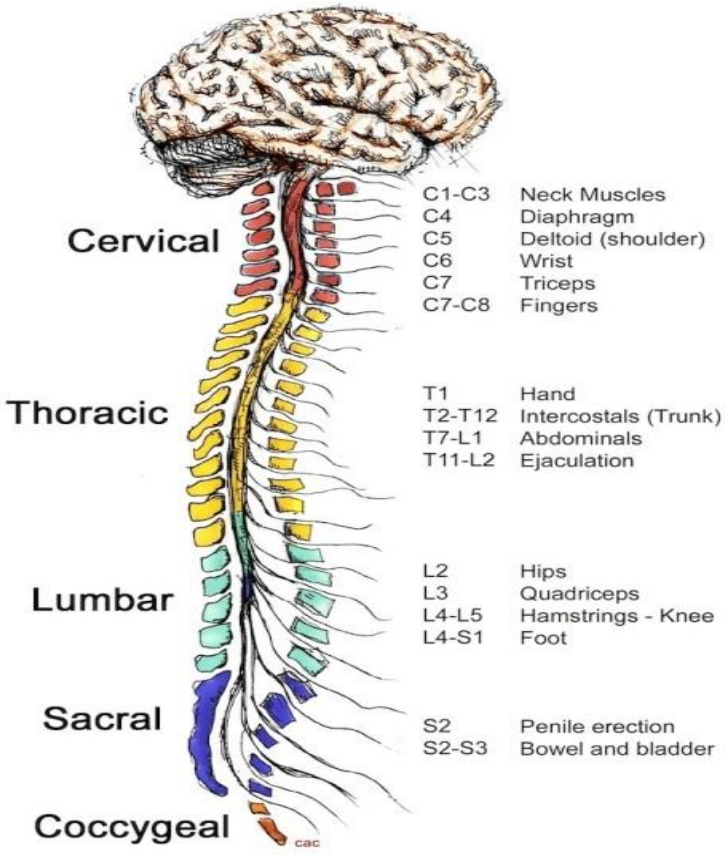

Figure 1-1 Central Nervous System of Mammals[2]

Neuroimaging can be classified into two broad categories:

Structural imaging [3] ,which tries to interpret the structure of the nervous system and deals with the diagnosis of intracranial disease and injury.

Functional imaging [4] , which is used to detect metabolic diseases, lesions, and also for neurological and cognitive psychology research and developing brain-computer interfaces.

The resultant images of neuroimaging techniques are not only useful to detect neurological diseases such as Tumours, Bleeding (which can be due to an injury), Blood clots, Inflammation, Birth defects, Stroke, Alzheimer's disease, Epilepsy, Dementia, Memory disorders but also leads researchers and doctors to understand the brain activities and helps to invert better techniques to identify the diseases at an early stage. The classified data collected from several neuroimaging process can be used to develop a database to record the patient's medical history to make more efficient machine learning algorithm which in turn can help the doctor to diagnose and predict the diseases from the feature symptoms[5].

1.2 Imaging Modalities

Due to the advancement of the technologies to collect neurological images of multidimensional and multi-parameterised data[6], it has been easier to visualise the medical data and compute several algorithms to ease the diagnosis by the physician. Bio-medical image processing

methods have been improved because of the advance technologies (including enhanced detector, instrumentation and computing methods) adapted to capture the physical parameters such as density, concentration, tissue properties, and surface area etc. of the biological data which leads to the decision parameters and information extraction algorithm of any knowledge based system.

Imaging modalities can be classified into three categories depending upon the experiment involved are Ex-vivo, In-vivo, and In-vitro imaging[7].

Ex-vivo refers to the experiment modality where the subject (organ, tissue, cell etc.) is placed outside the living organism and in a changed but controlled environmental conditions.

In-vivo refers to the experiment modality where the image is taken from a living or dead organism without changing its natural environment.

In-vitro refers to the experiment modality where the subject (organ, tissue, cell etc.) is cultured in a laboratory environment using test tubes, Petri dishes, etc.

Data gathered from several image modalities predicts the protein-protein interaction, neural networks, and dendritic spine topology and tries to improve the knowledge base.

The structural imaging technique includes methods such as CT (computed technology) scan, MRI (Magnetic Resonance Imaging) scan, Angiography. The functional imaging technique includes methods such as Positron emission tomography (PET), Electroencephalography,

Functional MRI, Transcranial magnetic stimulation (TMS), Magnetoencephalography.

The neuroimages used in the present work is collected by high resolution optical microscope. As images gathered from several different microscopic imaging tools differs in the parameters including depth of field, resolution and magnification of images, the comprehensive analysis of pathological and clinical data changes. Fluorescence microscopy, confocal microscopy, multiphoton microscopy, atomic force microscopy and electron microscopy come under microscopic imaging modalities.

Confocal microscopy[8] is an optical imaging technique that blocks all out of focus light using a small pinhole and considers only the reflected light from object in the focal plane to measure fluorescent properties of a specimen. Confocal laser scanning microscopy (CLSM) or laser confocal scanning microscopy (LCSM)[9] adds a laser to look over an object one pixel and one slice. This method is also useful for digitalisation of any 3D volume of data, obtaining high resolution slice by slice structures of ex-vivo or in-vivo cells, and investigating structural and morphological properties of living cells.

Furthermore, Multiphoton method[10] for confocal imaging technique uses in which the excitation wavelength is longer than the emission wavelength which results in near-infrared excitation light which can also excite dyes. This method can get the internal structure of a living tissue up to the depth of one millimetre. But multiphoton microscopy (two photons) exhibits limited temporal resolution. Stimulated Emission Depletion (STED) is a super resolution technique[11] which selectively deactivates the fluorophores, minimises the area of illumination at the

focal point, and thus enhances the achievable resolution (~30 nm). Electron microscopy reconstructs the topology of biological objects in their original states in 3D with resolution of ~5nm.

1.3 Mouse model to human model

Researchers and scientists greatly rely on Mice and rats for any clinical and pathological experiments[12]. One of many reasons is rodents are small, easily housed and can be maintained, and can adapt well to new surroundings. Their lifespan is short and they can reproduce easily, so several generations of mice can be observed in a relatively short period of time. There are a significant number of similarities as well as dissimilarities between human and mice but there share a common ancestor and have evolved through 100 million years which can be justified by the phylogenetic tree analysis by biologists. Researchers claim that the mammalian brain and nervous systems do share some genetic, structural and functional similarities. Mice exhibit same dendritic morphology as that of the human and share same social behaviour[13].Although the 5% genome structure differ from human but at sequence level, approximately, half of the human genomic DNA can be aligned with mouse genomic DNA. Like all mammalian species mice are prone to diseases like hypertension, cancer, diabetes and osteoporosis. But there are neurological diseases such as Cystic fibrosis and Alzheimer's[14] that affect humans but normally do not hit mouse. Mouse can be easily manipulated at genomic level and susceptible to environment change hence they are best choice for genetic engineering.

1.4 Motivation

- The challenge in neuro image processing lies in the process of image acquisition. The images captured through confocal microscopy shows problems like low contrast, low resolution and presence of noise etc. Also the choice of parameters involved in confocal laser microscopy is subjective in nature and expert's supervision is highly sought.
- In 3D image processing is computationally expensive and often researches prefer 2D neuro images for extracting dendritic morphology, spine density calculation of dendritic spine registration etc. The most popular algorithms including MIP, EDF etc. have their drawbacks such as high time complexity, data loss etc.; hence more accurate algorithm formulation is sought after.
- Optimum binariation is needed for skeletonization and automatic reconstruction of dendrite and dendritic spine in 3D.
- The 3D microscopic images of neuronal culture are highly intertwined and complex. In 2D projection image of this 3D volume, the structures often lead to misleading ideas about the spine distributions due to overlapping structures. The sub stack generation out of the overall volume stack for improved visualisation and accurate 2D projection is necessary henceforth.
- It is of great importance that the captured microscopic images align with the computational architectures as well as image processing methodologies. So approaches in solving these aforesaid problems are motivations leading this thesis.

1.5 Scope of Current Work

- Neuro Images shows noises due to the image acquisition modalities; in the proposed thesis and the built program module the noise minimizing filters are incorporated.
- The developed methods try to solve the problems of the data loss which occurs during Z-projection of any three dimensional image. Maximum Intensity Projection (MIP) is vastly used by the community of researchers and has its drawbacks. Two dimensional spine analysis[15] tools rely on MIP and their results can get better by using the proposed method, Locality sensitive Intensity Projection.
- Three-dimensional image binarization[16] is complex problem and for confocal microscopic images they produce inconsistent results. Proposed methods partially solve this problem and needs little expert intervention to collect the correct optimised data.
- Three dimensional neurological images show “Bridge” like structures in the 3D stack but visualisation[17] as well as slice by slice rendering can get complicated which leads to false interpretation of the cell morphology. The proposed method tries to generate multiple 3D images from one 3D image for better understanding.
- The scope of the thesis lies in the pre-processing of neuro images which in turn would help to achieve better results for the existing algorithms of 2D projection, skeletonization, Spine reconstructions in 2D dendritic spine analysis.

1.6 Organisation of the Thesis

In *Chapter 1,* we discussed the basic introduction of neurological image analysis and its importance in clinical, pathological research work and disease diagnosis. We elaborated the microscopic image modalities and discussed how rodent model resemblance with human model. We also discussed about the motivation behind this thesis and scope of this work.
In *Chapter 2,* we have done a brief survey of different on some classical image pre-processing modalities.

In *Chapter 3,* we have proposed the algorithm Locality Sensitive Intensity Projection (LSIP) and discussed in details and compared the result with the existing algorithm outputs.
In *Chapter 4,* we discussed about the three dimensional binarization techniques and analysed the result of the proposed method.

In *Chapter 5*, we explain the process of developing the GUI for pre-processing module for 3D images using basic QT GUI module. The steps to use the GUI are also including here.
In *Chapter 6,* an overall discussion of the work related to its advantage, shortcomings, future scopes are also discussed and concluded.

Chapter 2

Image Pre-processing Modalities

2.1 Noises of Neurological images

Various sources including external causes in transmission system and environmental factors can cause noises[18] in neurological images taken by confocal microscopes. Noises produce unwanted artefacts, unrealistic edges, blurred objects and unwanted information in digital images.

Noise model[19] can be broadly classified into following categories:

Gaussian Noise

Gaussian noise[20] follows the curve of probability distribution function of normal distribution. The mathematical formulation[21] is given below:

$$P(g) = \sqrt{\frac{1}{2\pi\sigma^2}}\, e^{\frac{-(g-\mu)^2}{2\sigma^2}}$$

Where σ is the standard deviation value, μ is the mean value, g is the grey-level intensity value.

Salt and pepper Noise

Due to the sharp and unexpected change in the input signal this type of noises[22] occurs in digital images. In low quality images high and low intensity data pixel values occurs in dark and bright regions respectively. Hence small dots of white pixel colour can be observed in dark

background and vice versa. The following diagram depicts the salt and pepper noise. The central pixel value is corrupted by pepper noise.

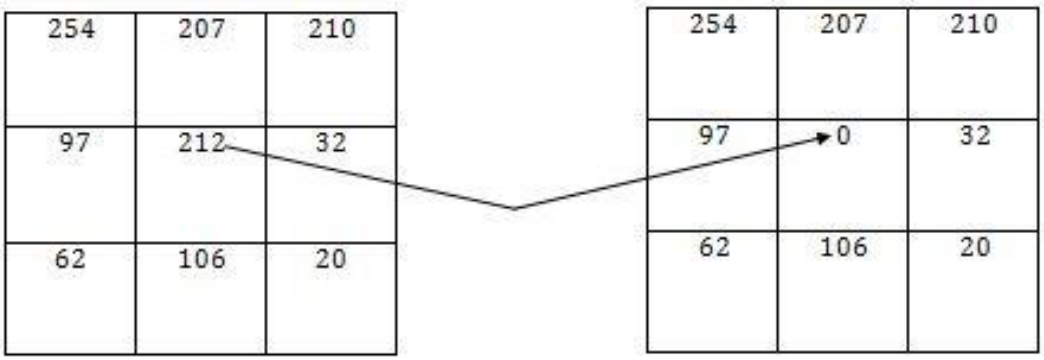

Figure 2-1Salt and Pepper Noise in Digital Images

Speckle Noise

Speckle noises[23] can be seen in MRI images mostly due to poor data signal transmission and produced by interfering echoes of a transmitted waveform originating from diversity of the studied objects. These noises are granular in nature present all over the images resulting degraded quality of images. This is a multiplicative noise and its probability distribution follows gamma distribution[24] .

$$F(g) = \frac{g^{\alpha-1}e^{-g/a}}{\alpha - 1!\, a^{\alpha}}$$

Where g is a grey-level intensity, α is the standard deviation value.

Poisson Noise

Poisson noise[25] occurs when the energy carrying partially slightly gives variation in transmitting medium and as the name suggests its probability distribution function follows Poisson distribution[26] .

$$P(f_{(Pi)}) = K * \frac{\lambda^K i^{e^{-\lambda}}}{K!}$$

Where K is the number of pixels considered or the number of event, λ is the mean value, e is Euler's constant.

Blurred Noise

Blurred noise[27] can be caused by low intensity and external factors. Images captured by hand held devices under low light give rise to this kind of noise.

2.2 Noises minimizing filters

Noise reduction mechanism[28] is a quintessential step for digital medical image processing. The images are prone to noise due to image acquisition process and it is very important to obtain mechanism to get rid of various types of noises which is again a subjective noise. Surgeons and doctors need improved multi-dimensional images for better diagnosis and disease detection. As we are going to propose several pre-processing algorithm for three dimensional data, hence 3D image filtering are of our subject of study.

Arithmetic Mean Filter

Arithmetic mean filtering[29] is a simple, easily implementable method of smoothing images. Smoothing reduces the amount of intensity variation between one pixel and the next. The idea is to replace each voxel intensity value by the mean intensity value of the neighbouring voxel and itself. Mathematically it can be presented as follows:

$$\hat{f}(x,y,z) = \frac{1}{mn} \sum_{(s,t)\in S} g(x,y,z)$$

Where S_{xyz} represent the set of coordinates in a cuboid sub image window (neighbourhood) of size $m \times n \times p$, concentrated at point(x, y, z), $g(x,y,z)$ is the source image and $\hat{f}(x,y,z)$ holds resultant values.

Mean filtering reduces the variance of any voxel's value with its surroundings and gives a blurred effect you the image. The mask for mean filter is given below:

$$g(i,j) = \frac{1}{3.3}\begin{bmatrix} 1 & 1 & 1 \\ 1 & 1 & 1 \\ 1 & 1 & 1 \end{bmatrix}$$

Median Filter

It is an order-statistics filtering mechanism[30] . In this process for each voxel the neighbourhood is checked and the median value is chosen. This method decides whether or not the pixel is representative of its surroundings.

$$f(x,y,z) = \underset{(s,t) \in S_{xyz}}{\text{median}} \{g(s,t)\}$$

Where $g(x,y,z)$ denotes the grey-level intensity value for the source image, and $f(x,y,z)$ denotes the output median filtered digital image.

Median filtering is effective in random noises and it shows relatively less blurring than arithmetic mean filtering. This method works well both for unipolar and bipolar noises. The formulation for median filter is given below:

$$g(i,j) = O_{m,n}[h(m,n)f(i-m,j-n)]$$

124	126	127
120	150	125
115	119	123

Figure 2-2Median filtering value calculation from a 3X3 window

Neighbourhood Values: 115, 119, 120, 123, 124, 125, 126, 127, 150

Median Value: 124

Gaussian Filter

Gaussian blurring filter[31] follows normal distribution function and its mathematical form is given below:

$$G(x) = \frac{1}{\sqrt{2\pi\sigma^2}} e^{-\frac{x^2}{2\sigma^2}}$$

For two dimensional images the formula would be

$$G(x,y) = \frac{1}{2\pi\sigma^2} e^{-\frac{x^2+y^2}{2\sigma^2}}$$

Where σ is the standard deviation of the distribution is, G(x, y) denotes the distance from origin in horizontal and vertical directions. Values from this distribution can be useful to build a convolution matrix. Each pixel's new value is set to a weighted average of that pixel's neighbourhood. The original pixel's value receives the heaviest weight (having the highest Gaussian value) and neighbouring pixels receive smaller weight as their distance to the original pixel increases. This results in a blur that preserves boundaries and edges better than other, more uniform blurring filters:

$$g(i,j) = \begin{bmatrix} 1 & 4 & 7 & 10 & 7 & 4 & 1 \\ 4 & 12 & 26 & 33 & 26 & 12 & 4 \\ 7 & 26 & 55 & 71 & 55 & 26 & 7 \\ 10 & 33 & 71 & 91 & 71 & 33 & 10 \\ 7 & 26 & 55 & 71 & 55 & 26 & 7 \\ 4 & 12 & 26 & 33 & 26 & 12 & 4 \\ 1 & 4 & 7 & 10 & 7 & 4 & 1 \end{bmatrix} \qquad \text{Where } \sigma^2 = 2, \text{i , j} = 7.$$

Chapter 3

Locality Sensitive Intensity Projection

3.1 Literature Survey

Maximum Intensity Projection

Maximum Intensity Projection[32] is a method which projects the maximum intensity value that comes along the way of the ray traced from the upper layer to the bottom layer of the 3D image stack. Essentially the 2D image or projection resulting from this algorithm holds the maximum intensity of the voxel mapped to the pixel.

The main drawback[33] is highly discontinuous index map which means that the consecutive pixel information may belong to two voxels from different layers of the image stack. So it can be said that MIP does not depict depth relationship and convey actual information of overlapping structures. Structures having higher intensity values behind lower values structure would appear in front of them in 2D projection.

Extended Depth Field Method

In extended depth field[34] method the idea is to merge a stack of 2D images, which are taken at different focal positions into a single but entirely focused composite image. Here the focal length of a projector is periodically changed and this fast change in focal length results in forward and backward sweeping of focal length which in turn makes the point spread function of each pixel projected integrate. This approach

uses wavelet transform, which uses selection rule based on maximum absolute coefficient.

All though in this method the issue of discontinuous index map is addressed but it mainly results a smooth index map but does not pass any judgement on foreground and background data identification.

As colour channels are independently processed in a systematic manner here it is not taken into account.in the resulting image one colour pixel can be made up of colour component of different voxel at different level.

This method is not parameter free and this can be said to be subjective choice[35].

Smooth Manifold Extraction

Smooth Manifold Extraction[36] maintains continuous index map obtained from single channel in the projection both within the channel and also between different channels. This method identifies the foreground information among the background details. The local variance ensures smooth index map.

$$Z^* = W \times H \subset N^2 \rightarrow D \subset R \text{ [This tries to find optimal map]}$$

By solving,

$$Z^* = \underset{Z}{argmin} \sum_{(x,y)} c(x,y)\,|Z_{max}(x,y) - Z(x,y)| + D_Z(x,y)$$

Z_{max} = Maximum focus map having weighted class map C and the local spatial standard deviation σ_Z

$$Z_{max}(x,y) = \underset{Z}{\text{argmax}} F(x,y,Z)$$

$$F(x,y,Z) = \begin{cases} I(x,y,Z) \text{ for confocal image} \\ SML(G * I(x,y,Z) \text{for widefield image} \end{cases}$$

$I =$ input image

$SML =$ sum of modified Laplacian

$G =$ Gaussian Filtering

Calculation of weighted index map:

$F_Z(x,y)$ is a 2 D volume manifold , $P_Z(x,y)$ is a power spectra and formulated as

$$P_Z(x,y) = |FFT(F_Z(x,y))|^2$$

$FFT =$ Fast Fourier Transform.

Calculating class-specific control:

$$c(x,y) = \begin{cases} c_P \text{ if } P_Z(x,y) \text{ belongs to foreground class} \\ c_V \text{ if } P_Z(x,y) \text{ belongs to uncertain class} \\ 0 \text{ if } P_Z(x,y) \text{ belongs to background class} \end{cases}$$

Calculating local spatial Standard Deviation:

σ_x is computed over a 3×3 window around each pixel (x,y) in the cost function to minimize. This ensures the smoothness. The algorithm is stated below:

SME is a time consuming process and susceptible to noise. This algorithm doesn't produce optimal result for confocal microscopic images.

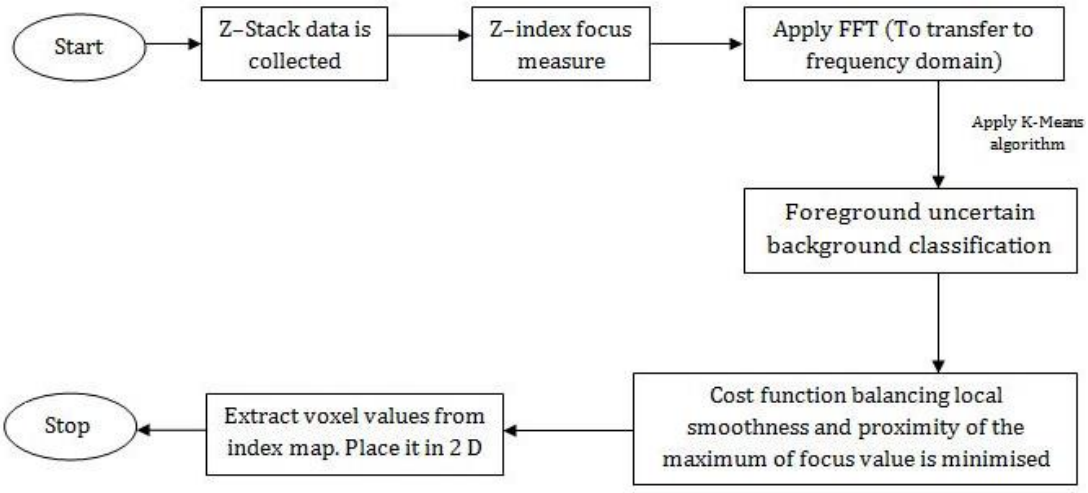

Figure 3-1 Flow Chart of Smooth manifold extraction Algorithm

3.2 Research Gap

It can be said that MIP does not account the problem of spatial consistency and for detailed and fine microscopic structure it generates misleading result. MIP can give below average result for noisy result.

EDF projection is a subjective choice because adjusting the pinhole and taking multiple images of live cells needs expert's supervision.

SME creates continuous index map but it does not account for noise and it is time consuming.

3.3 LSIP Algorithm

Locality Sensitive Intensity Projection is an advance approach to solve the rudimentary problem associated with the 2D projection of any 3D volume.

Studies show that in case of the confocal microscopic neuro-images depending upon the pinhole optimisation of the device the images vary

greatly. However, it is common that the rays converge at the focal point of the lens, resulting the image clearer at the middle layer of the volume stack. So the upper and lower layers of the stack are very much susceptible to noise.

Here two statistical assumptions are taken to establish the algorithm.The algorithm considers that the standard deviation should be high between the background and the foreground data of the image stack.The second presumption is that the standard deviation between two adjacent voxel should be very low at the data region.

Standard deviation show the range of the data spread in a given region. A low standard deviation value indicates that the data points tend to be close to the mean of the data set, while a high standard deviation value indicates that the data points are spread over a wider range of the values. The algorithm (Figure: 3-2) is stated here below:

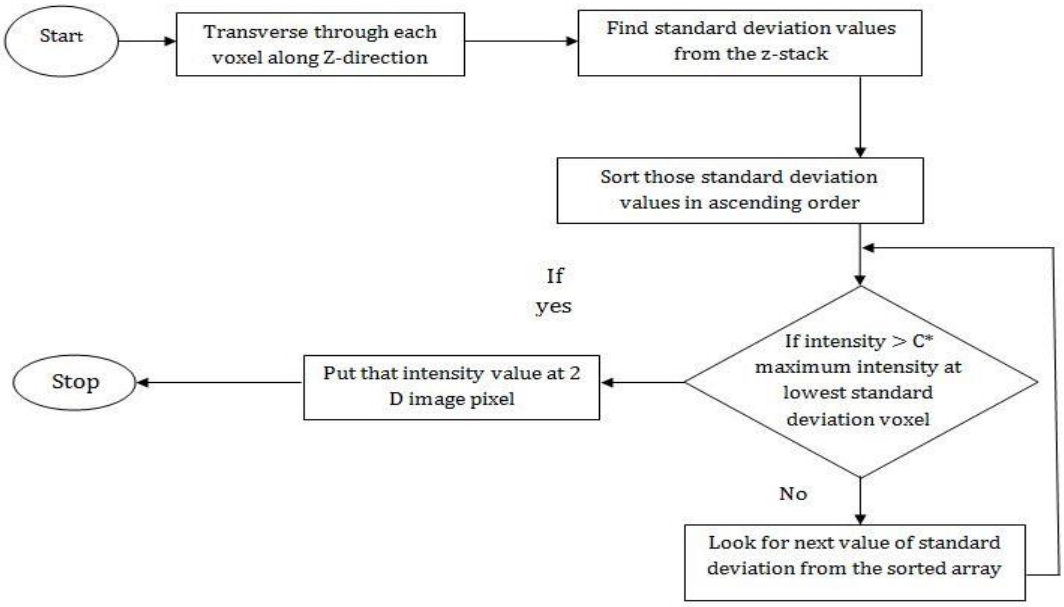

Figure 3-2 Flow Chart of Locality Sensitive Intensity projection

The fundamental idea is to optimise the result of Maximum Intensity Projection. A ray is traced from the upper to lower layer of the stack examining the standard deviation value of each voxel with respect to its neighbours and the intensity. The goal is to find the minimum standard deviation of such a voxel in traversal which holds the c% of the maximum intensity of that pass.

This technique significantly reduces noise and produces continuous index map.

On contrary to existing methods this method generates optimised results on neuro-images upon changing two parameters, i.e. the neighbourhood window size and the intensity tuning factor(c).

3.4 Result Analysis

It is evident form (Figure 3-3, 3-4, 3-5), that the developed method Locality sensitive Intensity projection significantly reduces noise in the 2D projection keeping the relevance of the 3D data intact. The background and foreground identification is also optimal.

Figure 3-6 shows that LSIP algorithm can be more efficient if the window size taken for locality sensitivity is larger. The figure 3-6 shows the result of the several projections keeping the window size 5*5*5 voxel.

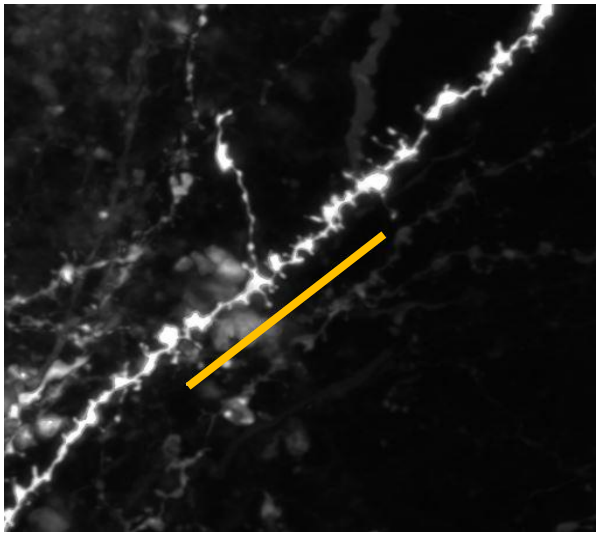

(a)

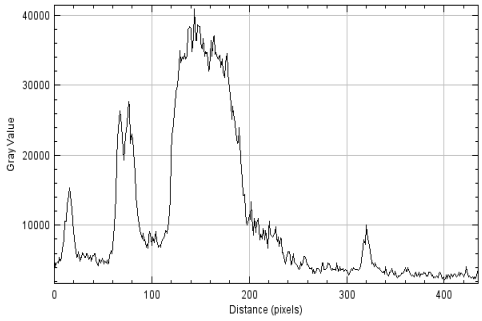

(b)

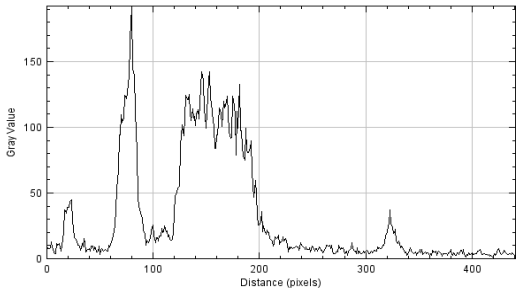

(c)

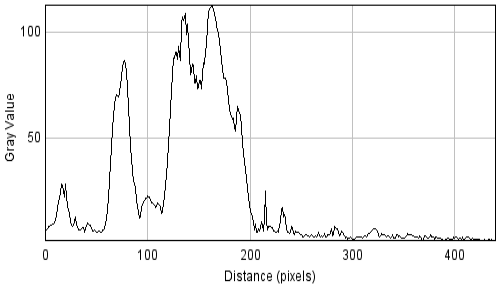

(d)

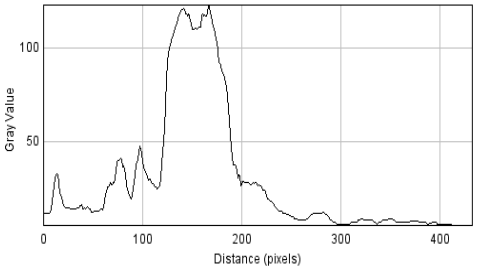

(e)

Figure 3-3(a) Section of image projection (b) MIP Plot Profile,(c) EDF plot profile, (d) SME Plot Profile,(e) LSIP plot profile

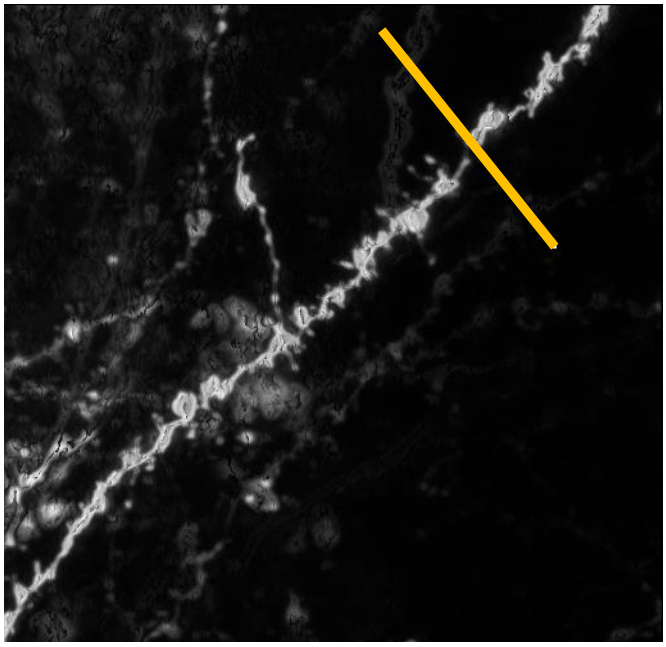

(a)

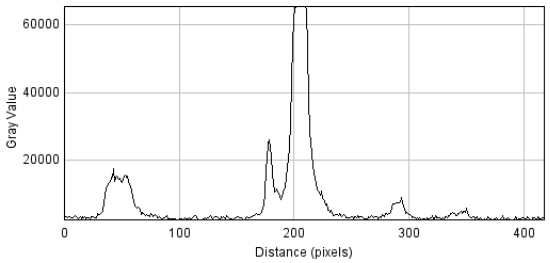

(b)

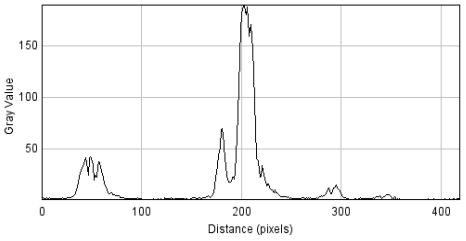

(c)

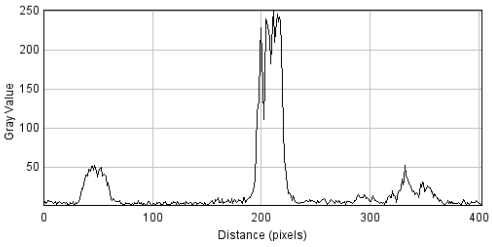

(d)

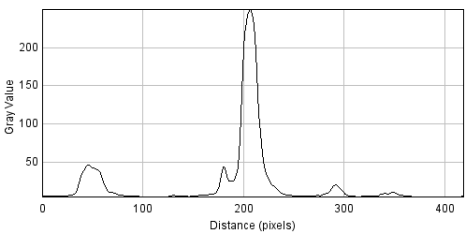

(e)

Figure 3-4(a) Section of image projection (b) MIP Plot Profile,(c) EDF plot profile, (d) SME Plot Profile,(e) LSIP plot profile

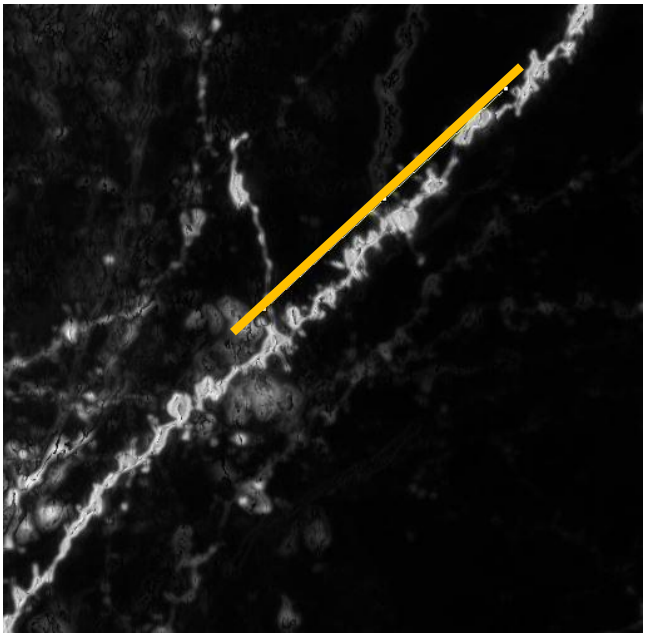

(a)

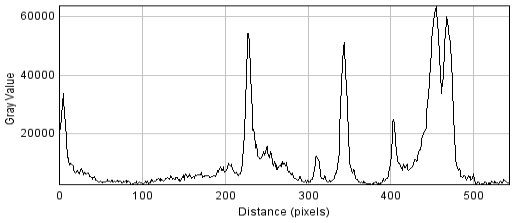

(c)

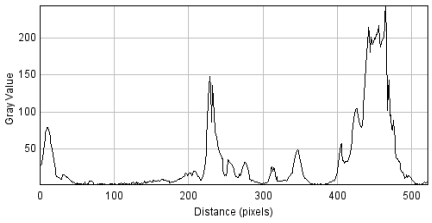

(d)

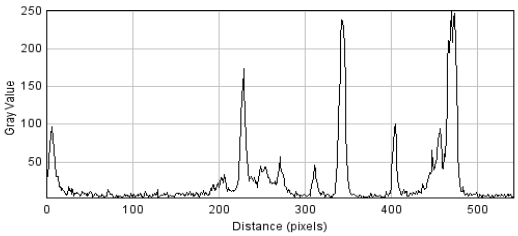

(e)

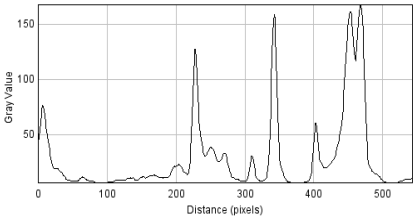

(f)

Figure 3-5a) Section of image projection (b) MIP Plot Profile,(c) EDF plot profile, (d) SME Plot Profile,(e) LSIP plot profile

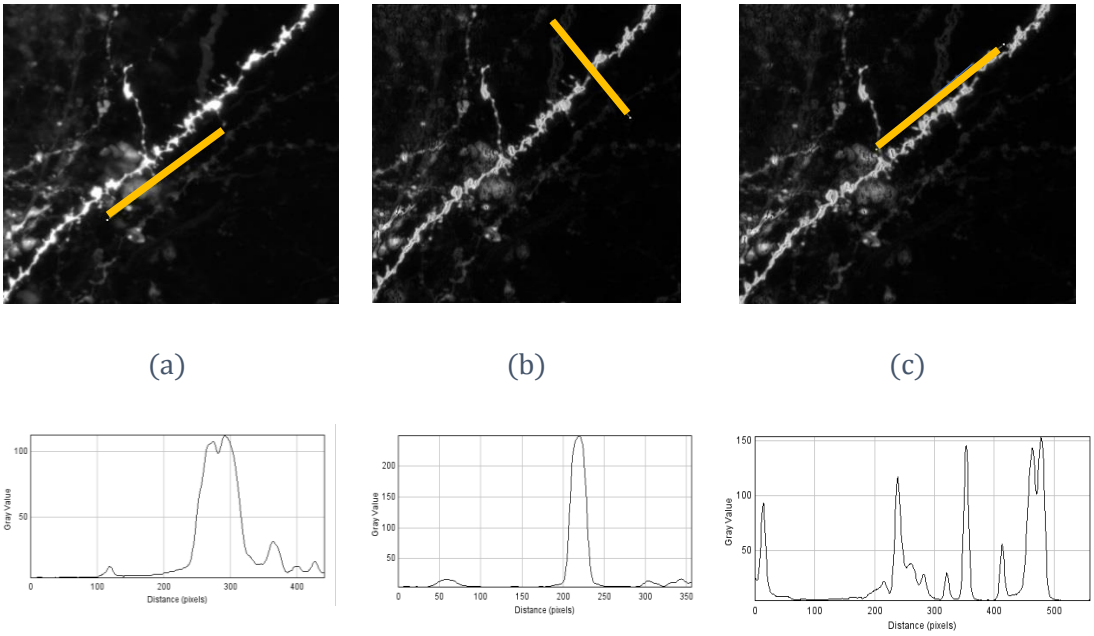

Figure 3-6 (a),(b),(c) shows selected line on the projection taking,(d),(e),(f) show the LSIP plot profile for the same respectively

Chapter 4

3D Binarization

Image binarization[37] is a technique of image processing which converts grey-scale image into a binary image. Hence only one bit is sufficient to represent one voxel. Although binarization does not deliver accurate and high quality data due to poor source type and the image acquisition process but however, this process essentially contributes to the identification of foreground and background data. For neurological image processing binarization can lead results which will depict the basic structures of the dendritic spines closer to the actual cell.

In case of microscopic images the data volume is a 3D stack which contains multiple layers hence finding the background and foreground data is more complex. Identification of noise in the foreground is necessary for accurate result.

On contrary to 2D image binarization[38], 3D image binarization will be more complex as the resultant binary image will contain noise even more at the upper and lower layer of the stack. So, it is important to find to choose a binarization method that restricts erroneous pixels from becoming the subject for processing and potential cause of errors for post-processing steps.

4.1 Literature Survey

Image Binarization is also known as Image Thresholding[39]. It simply separates the region which holds the intensity value higher than the set

threshold. Binarization can be done in two classical ways: Global Thresholding and Local Thresholding.

In case of global thresholding[40][41] a fixed intensity value is considered as threshold for the whole image. The pixels containing higher intensity than the said threshold will be set as bright regions and the pixels containing lower intensity value lower that the said threshold will be set as dark region.

In case of local thresholding[42], for every pixel adaptively local threshold is calculated within a given window size.

Few Global Thresholding techniques are as follow: Fixed Thresholding Method, Otsu's method.

Few Local Thresholding techniques are as follow: Adaptive Binarization, Ni-Black method, Sauvola Method, Brennsen method.

Fixed Thresholding Technique

In fixed thresholding technique[43] one global threshold value is considered to assign 0's and 1's to every voxel position of the 3D volume. The basic formulation is given below:

$$b(x,y,z) = \begin{cases} 1 \text{ if } g(x,y,t) > C \\ 0 \quad \text{otherwise} \end{cases}$$

Where $b(x,y,z)$ is the binary intensity value at voxel(x, y, z), $g(x,y,z)$ is the grey-level intensity value, C is a fixed global grey level intensity value.

Now, setting threshold intensity for complex images is a subjective choice and hence this is not an optimised method.

Otsu's Method

This method[44], depending on the shape of the histogram, is used for automatic binarization level decision. Otsu's thresholding method calculates all the possible threshold values iteratively and calculates a measure of spread for the voxel levels each side of the threshold value to check if the voxel falls in foreground or background. The goal is to find that threshold where minimum value of the sum of foreground and background spreads is.

Local Adaptive Binarization

In this technique instead of a global threshold a local threshold is calculated by scanning the whole image by an N*N*N block. This window slides over the image and calculates the local threshold for that particular centre voxel. This technique essentially gives optimised and meaningful information when the image is affected by blurring, low resolution. The local threshold calculation can be done by Ni-Black, Sauvola or Bernssen method.

$$b(x,y,z) = \begin{cases} 0 \text{ if } g(x,y,z) \leq T(x,y,z) \\ 1 \qquad \text{otherwise} \end{cases}$$

Where $b(x,y,z)$ is the binary intensity value at (x, y, z) voxel, $g(x,y,z)$ is the grey intensity value at (x, y, z) voxel, $T(x,y,z)$ is calculated threshold value for binarization.

Ni-Black Method

In this technique[45] the standard deviation and the mean of the intensity values of the window of size N*N is calculated. Depending on these value the following formula to calculate the threshold-

$$T(x, y, z) = m(x, y, z) + k * S(x, y, z)$$

Where $T(x, y, z)$ is the threshold intensity calculated at (x, y, z) voxel, $m(x, y, z)$ is the mean intensity value around (x, y, z) voxel within the window size, S(x, y, z) denotes the standard deviation value of voxel (x, y, z) around N*N window, k is a bias and gives satisfactory result at -0.2.

Sauvola Method

This technique[46] is a modified form of Ni-Black technique as the idea of calculating standard deviation and mean in the N*N window is same but the formula is different which is used to calculate the threshold. The formulations are given below-

$$T(x, y, z) = m(x, y, z) * \left[1 - K * \left(\frac{S(x, y, z)}{R} - 1\right)\right]$$

Where $T(x, y, z)$ is the threshold intensity calculated at (x, y, z) voxel, $m(x, y, z)$ is the mean intensity value around (x, y, z) voxel within the window size, S(x, y, z) denotes the standard deviation value of voxel (x, y, z) around N*N window, R denotes the dynamics of standard deviation fixed to 128 and K refers to a fixed value of 0.5.

Brenssen Method

Brenssen Method is a simple local binarization technique where the threshold intensity value of each pixel will be computed from the values of its neighbouring pixels. The formula is given below-

$$T(x, y, z) = 0.5(I_{max}(x, y, z) + I_{min}(x, y, z))$$

Where $T(x, y, z)$ is the threshold intensity calculated at (x, y, z) voxel, $I_{max(x,y,z)}$ and $I_{min}(x, y, z)$ are maximum and minimum grey values within the local window provided contrast:

$$[C(x, y, z)] = I_{max}(x, y, z) - I_{min}(x, y, z) \geq 15$$

$$b(x, y, z) = \begin{cases} 0 & \text{if } m(x, y, z) < T(x, y, z) \\ 1 & \text{otherwise} \end{cases}$$

Where $T(x, y, z)$ is the threshold intensity calculated at (x, y, z) voxel, $m(x, y, z)$ is the mean intensity value around (x, y, z) voxel within the window size, $g(x, y, z)$ is the grey-level intensity calculated at (x, y, z) voxel, $b(x, y, z)$ is the threshold intensity calculated at (x, y, z) voxel,, S(x, y, z) denotes the standard deviation value of voxel (x, y, z) around N*N*N window.

4.2 Developed Algorithm

The basic idea is to design an efficient technique where the binarization of 3D stack is based on the approaches used in 2D binarization[47]. To develop the binarization threshold for any complex biological data it is important to simultaneously identify the foreground and background data. Most of the laser microscopic images are prone to noises hence it is important to reduce those noises by using filters.

This method(Figure: 4-1) uses Mean Filtering on the grey-scale data to minimize the noises and uses the locality sensitivity to calculate the standard deviation in each voxel with respect to its N*N*N 3D window. The resultant of the mean filter holds the grey-scale intensity, and the standard deviation value calculated for each pixel with respect to the neighbouring pixel in the window size N*N*N is stored . One

predetermined constant C is taken into account and the subjective choice of the value of the constant is ideally between 1 and 2.

The proposed formula for local thresholding of each voxel is by the following formula:

$$T(x, y, z) = S(x, y, z) * C * g(x, y, z)$$

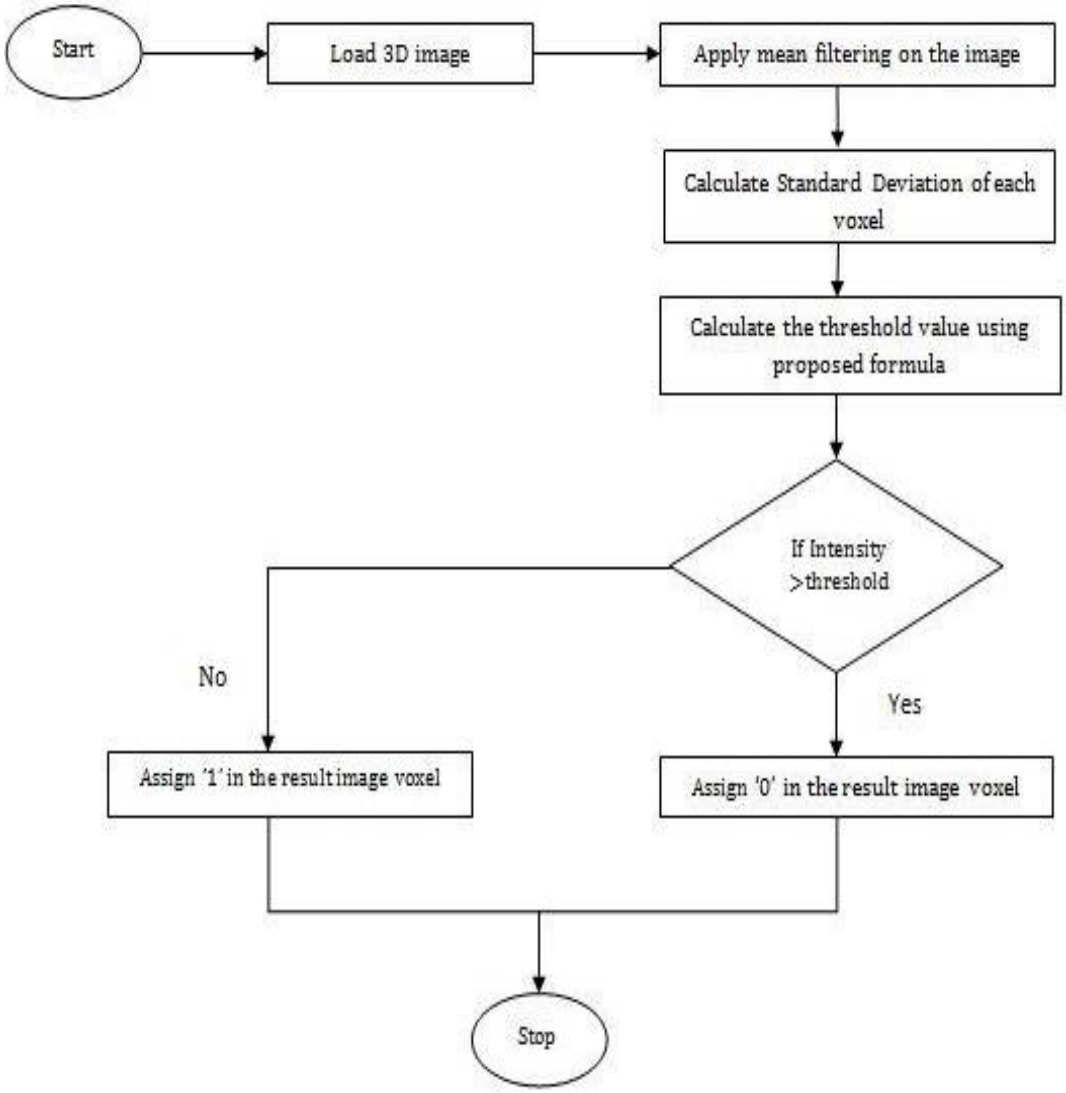

Figure 4-1 Flowchart for proposed algorithm of 3D Binarization

4.3 Result Analysis

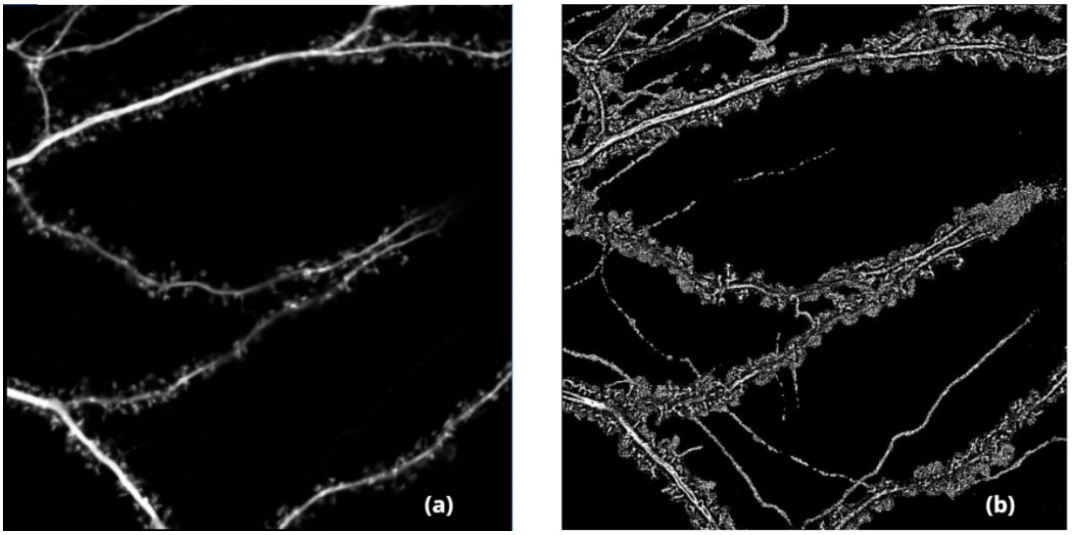

Figure 4-2 (a) Original image of Dendritic Spine at its middle layer, (b) Binarized image of (a) using Ni-Black Method

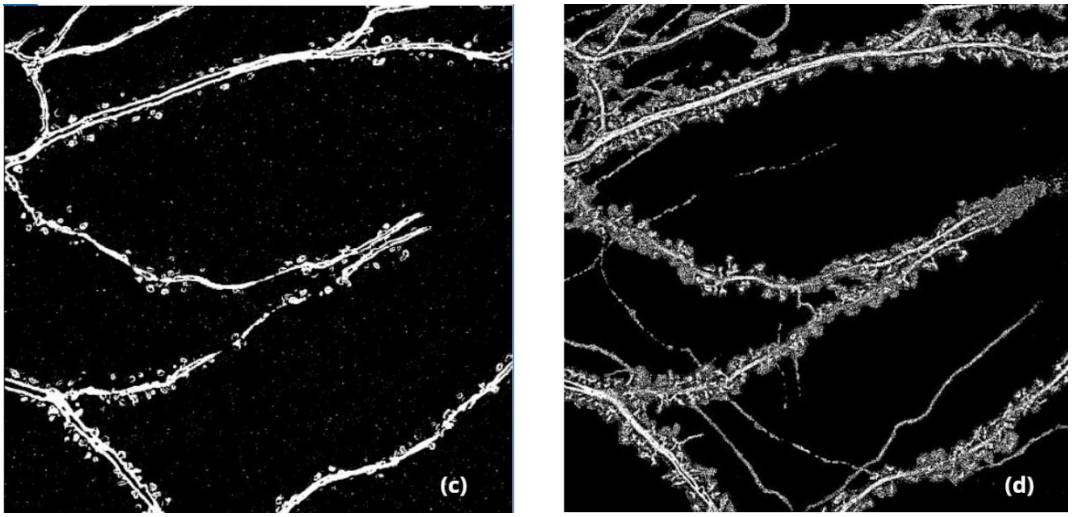

Figure 4-3(c) Binarized image of (a) using Sauvola Method, (d) Binarized image of (a) using Brenssen Method

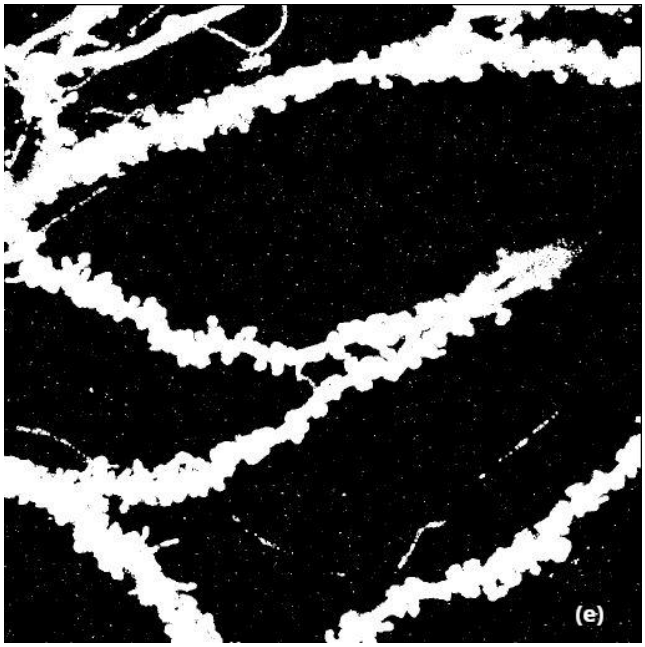

Figure 4-4 (e) binarized imaged of Figure4-1(a) using proposed method

An algorithm is designed for local thresholding and analysed the obtained results with Ni-Black, Sauvola, and Brenssen methods. As the result is a 3D volume and we predominantly analyse the most relevant data hence for simplicity only one layer from middle of 3D binary volume is shown here. It is observed that due to binarization by the aforesaid techniques some data are lost and original protrusions around the dendritic spines are not preserved its shape.

4.4 Conclusion

The algorithm is designed for local thresholding and analysed the obtained results with Ni-Black, Sauvola, and Brenssen methods.

Because the result is a 3D volume, for simplicity only the middle layer of the 3D volume is projected here and it is evident that all the aforesaid

methods are not information preserving and the protrusions are not coherent with the actual structure.

The proposed method is easy, effective and generates optimised result from 3D volumes. The spine morphology depicted in the binarized image is comparable to that of the original 3D volume.

Chapter 5

Dynamic Image partitioning

3-Dimensional images are a stack of several 2D images and difficult to render or process[48]. Confocal light microscopy images of dendritic spines are one of the most complex 3D data while cancer cells[49], microscopic images of several tissues show very complex 3D structures.

Due to overlapping bridge like dendritic spine structure the 3D to 2D conversion algorithms do not give satisfactory results. The misleading information comes from the noisy non-data part of those images.

Any further processing on the 3D data is prone to data loss and algorithmically complex. So an automatic algorithm would help the biologists to identify different layers of such a complex 3D volume which somehow hide any morphological structure[50] behind it.

Our proposal would divide that complex image stack into multiple 3D volumes which would contain the original data and would be helpful to the subject experts.

5.1 Developed Algorithm

Step 1: The maximum Intensities along Z-axis is calculated for every voxel.

Step 2: If the voxel intensity is greater than the set threshold then we consider that particular voxel to be part of our information cluster.

Step 3: Find that Z layer where the information cluster count hit is maximum.

Step 4: Find those layers where the information cluster hit is greater than a pre-set value (which is comparable to the image's X and Y dimensions). And mark those layers to be part of multiple 3D data volumes.

Step 5: The layers which are not part of such clusters are the break points of 3D images.

Step 6: Slice the image along Z volume wherever the breakpoints are encountered.

5.2 Result Analysis

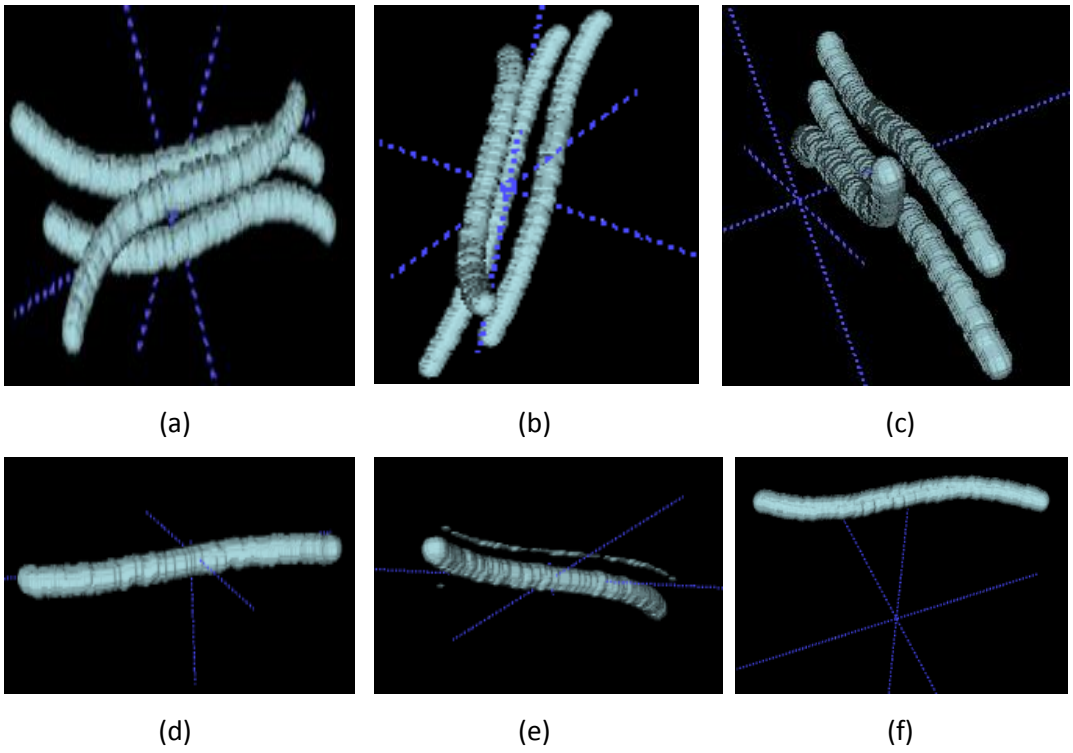

Figure 5-1 (a),(b),(c),(d) show 3D visualization of Synthesised data from different plane,(e), (f), (g) show the segmented phantoms

It can be observed from the above result image that our proposed algorithm dynamically partitioned one 3D volume resulting multiple 3D

images with maximum information in every volume. The results are of synthesised phantoms and depicted as 3D segmentation. The original image shows in (Figure: 5-1(a),(b),(c),(d),(e),(f)) a complicated image with intervening 3 phantoms in Z plane. Our algorithm successfully divided the phantoms into 3 images and gives better visualisation of the 3D volume.

5.3 Conclusion

It can be concluded that our algorithm effectively identifies the data from the background in every x-y plane. The plane with maximum information having background plane in between can be considered as the terminal slice of one given volume. Thus our algorithm considers a plane with less information adjoining two planes with maximum possible information as the plane of division.

The resultant image can be used for 3D spine analysis and can be subjected to our proposed 2D projection algorithm, Locality Sensitive Intensity Projection, to observe more accurate spine structures and to analyse the same.

Chapter 6

Development of the GUI

6.1 Introduction of QT GUI

Qt[51] is a cross-platform framework usually used as design graphical user interface and application. It provides system integration, event handling, OpenGL and OpenGL ES integration, 2D graphics, basic imaging, fonts and text. It provides programmer friendly environment and does not requires high level training. Mainly Qt IDE is in C++ but one can integrate OpenCV, python with Qt if required.

For application developers writing user interfaces, Qt provides higher level API's, like Qt Quick, that are much more suitable than the enablers Qt GUI module

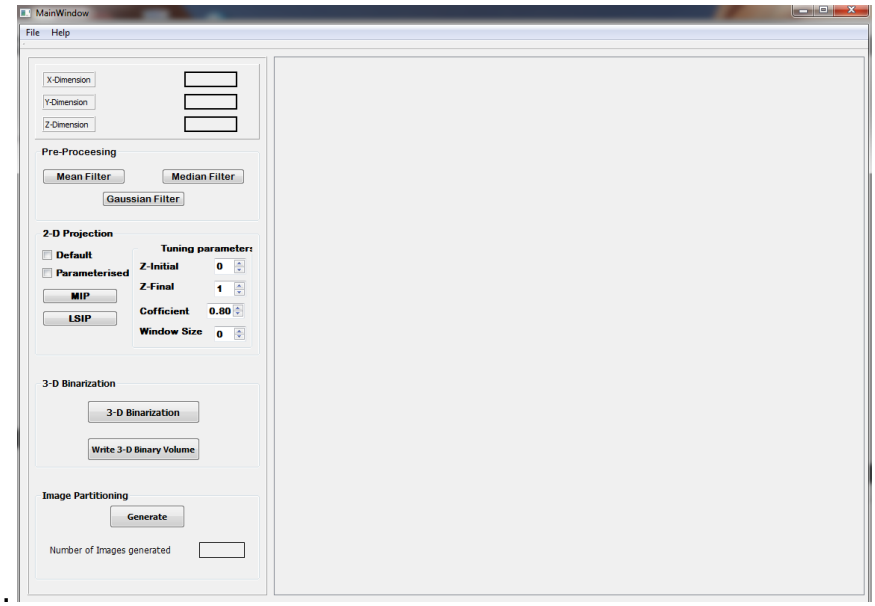

Figure 6-1 GUI of the pre-processing application

6.2 User Manual

In this Section we are going to discuss about the GUI (Figure 6-1) for our proposed algorithm.

The Load Image(Figure: 6-1) option upon clicking enables users to select any 3D data. The Save Image option upon clicking user can save 2D image files into the disk.

Pre-processing

Button Mean Filtering**:** On clicking this button (Figure: 6-1) 3D mean filter will be applied on the chose 3D image.

Button Median Filtering**:** On clicking this button (Figure: 6-1) 3D median filter will be applied on the chosen image.

Button Gaussian Filtering**:** On clicking this button (Figure: 6-1) 3D Gaussian filter will be applied on the chosen image.

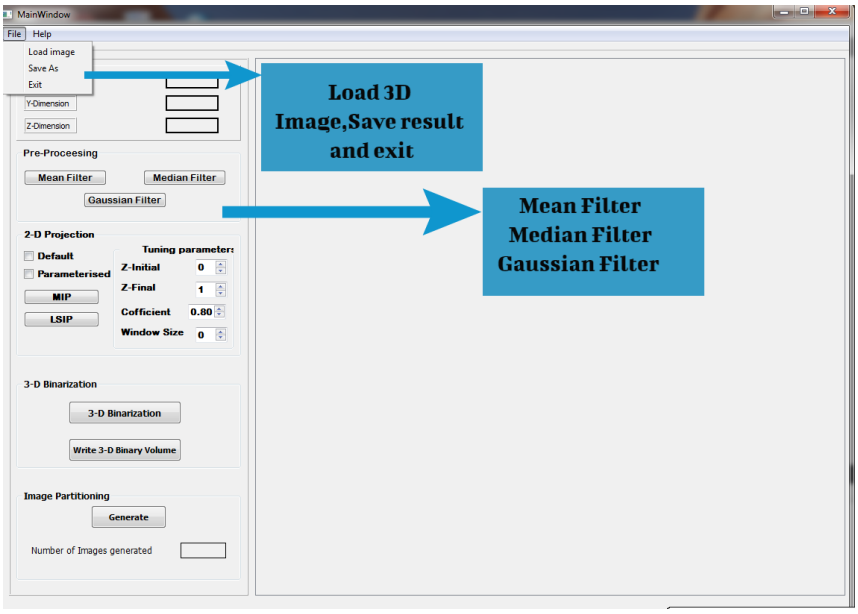

Figure 6-2 Options and Button functions

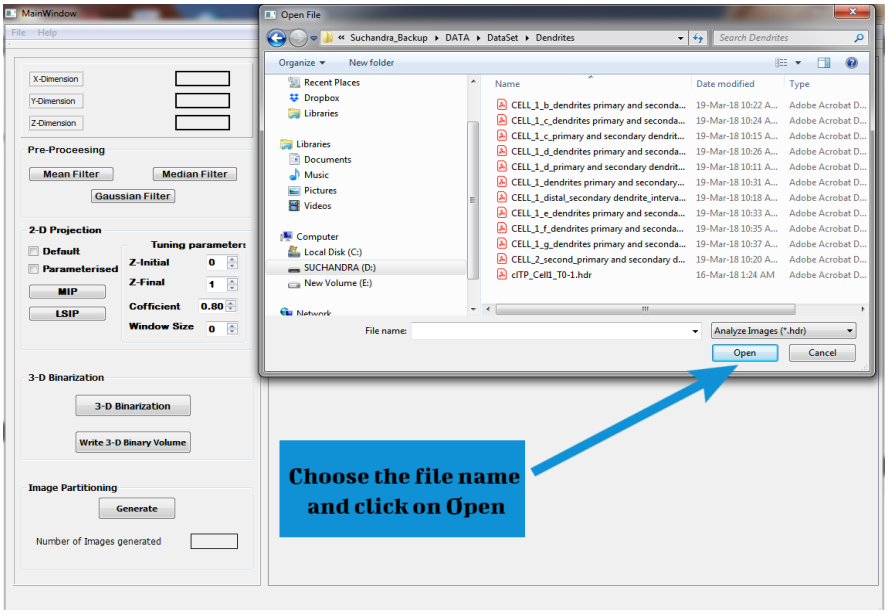

Figure 6-3 On Load Image clicked

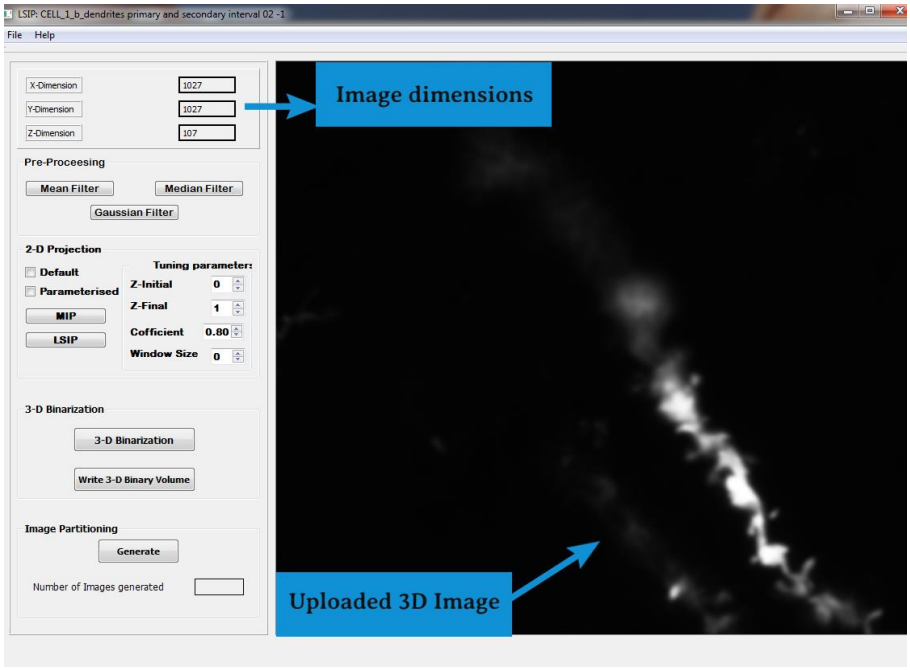

Figure 6-4 Uploaded 3D image in the GUI

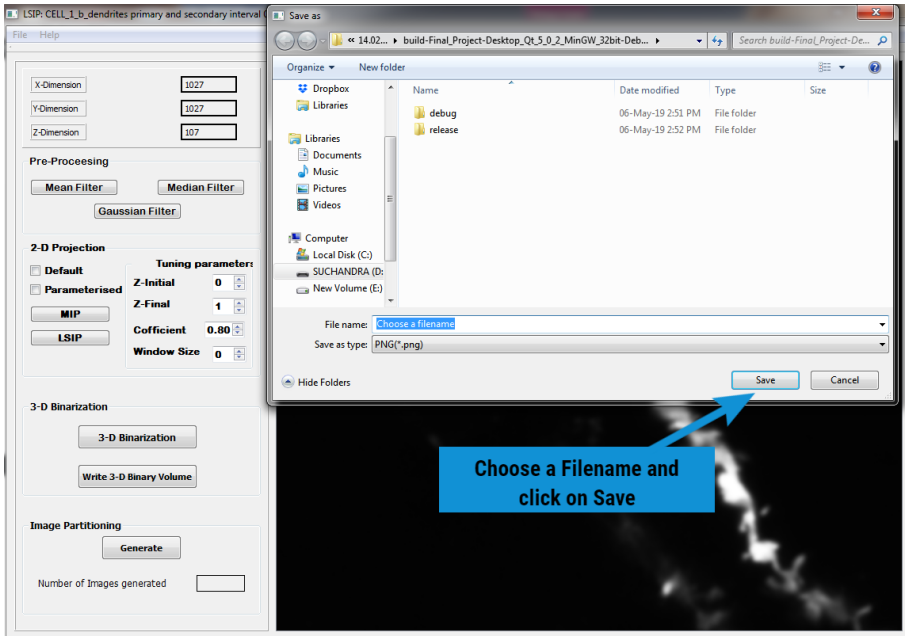

Figure 6-5 on Save clicked

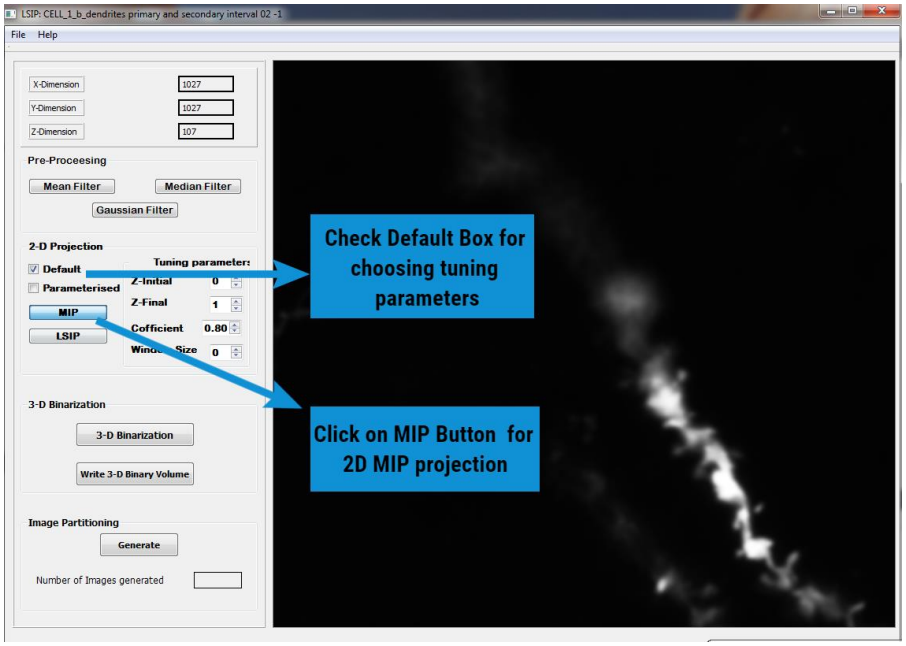

Figure 6-6 Default MIP button clicked

2D Projection

Button MIP: In default mode (Figure: 6-6, Figure: 6-7) the maximum intensity projection is done on the overall stack. In parameterised mode user can manually change the tuning parameters and get the MIP result.

Button LSIP: In default mode (Figure: 6-8, Figure: 6-9) the Locality sensitive intensity projection is done on the overall stack. In parameterised mode user can manually change the tuning parameters and get the LSIP result.

3D binarization

Button 3D Binarization: On clicking this button (Figure: 6-10) 3D binarization algorithm run on the loaded 3D image.

Button 3D Binary volume: On clicking this button the generated 3D image stack is written in an .img file in debug folder of the project.

3D Partitioning

Button Generate: On clicking this button (Figure: 6-11) multiple 3D image will be generated from a given image stack.

Textbox No. of image generated: the number appears inside the text box indicates the number of image generated by the algorithm.

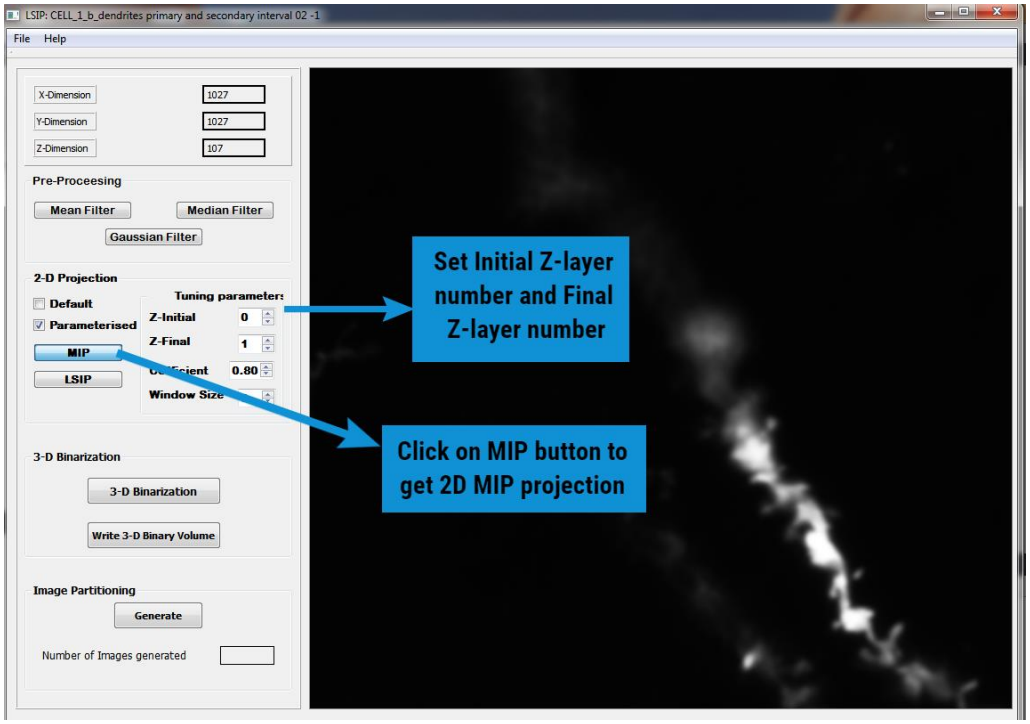

Figure 6-7 Parameterised MIP button clicked

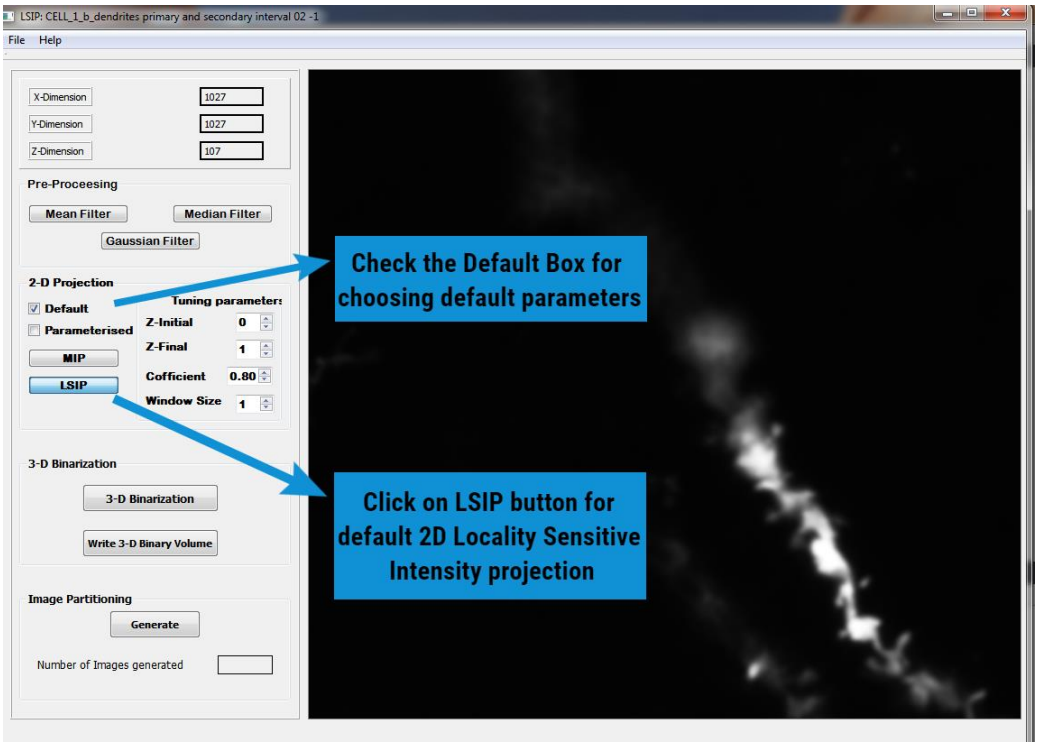

Figure 6--8 On Default LSIP button clicked

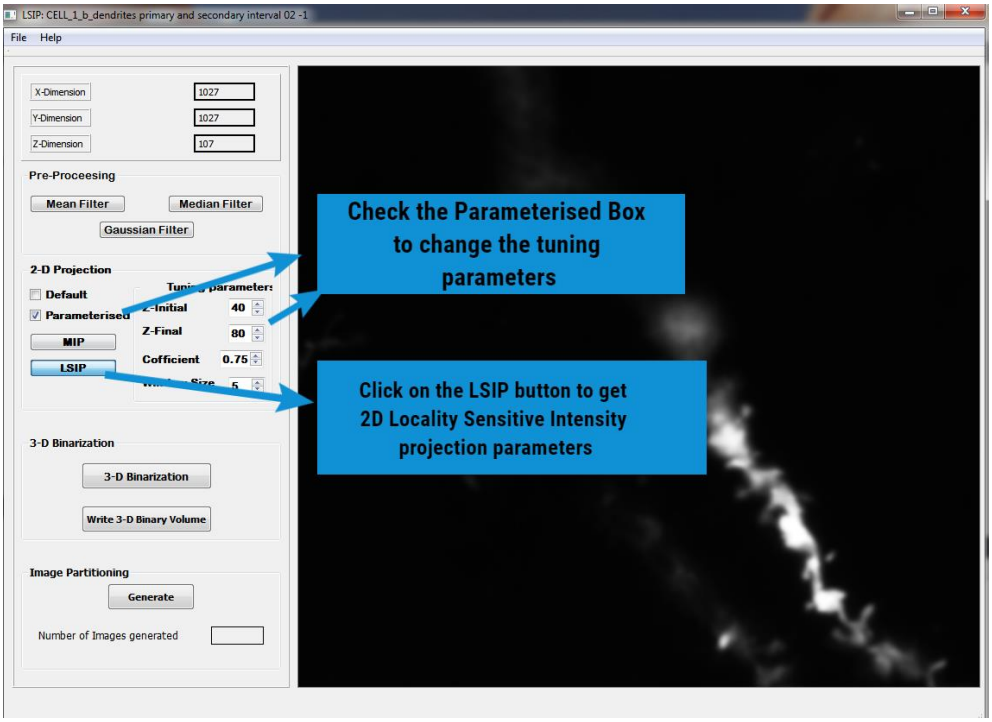

Figure 6-9 On Parameterised LSIP button clicked

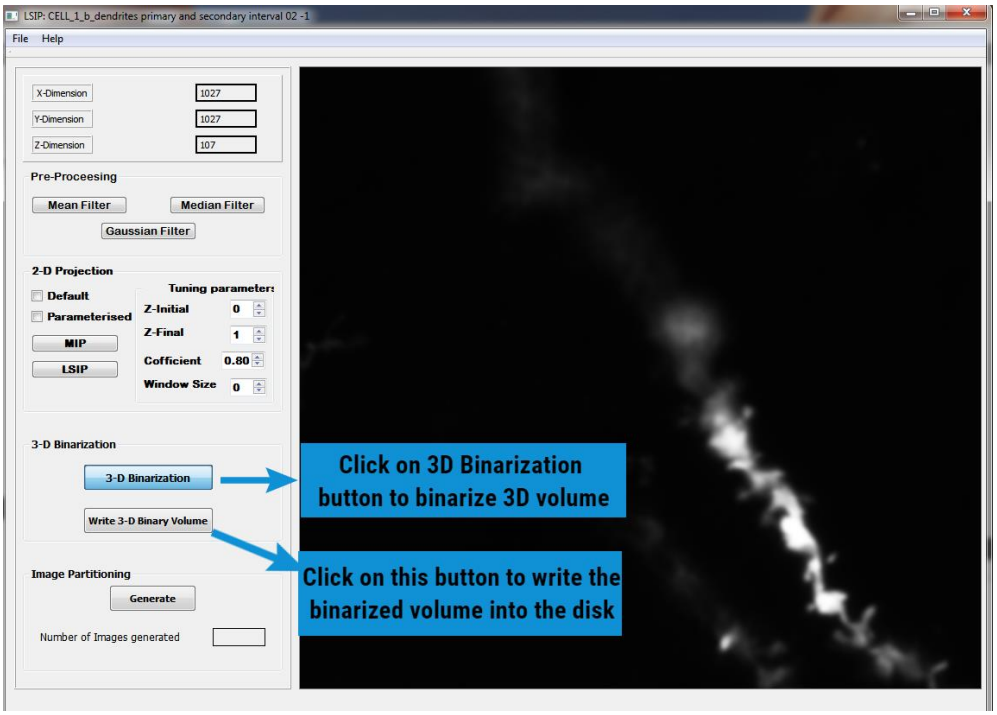

Figure 6-10 3D Binarization and Write Button clicked

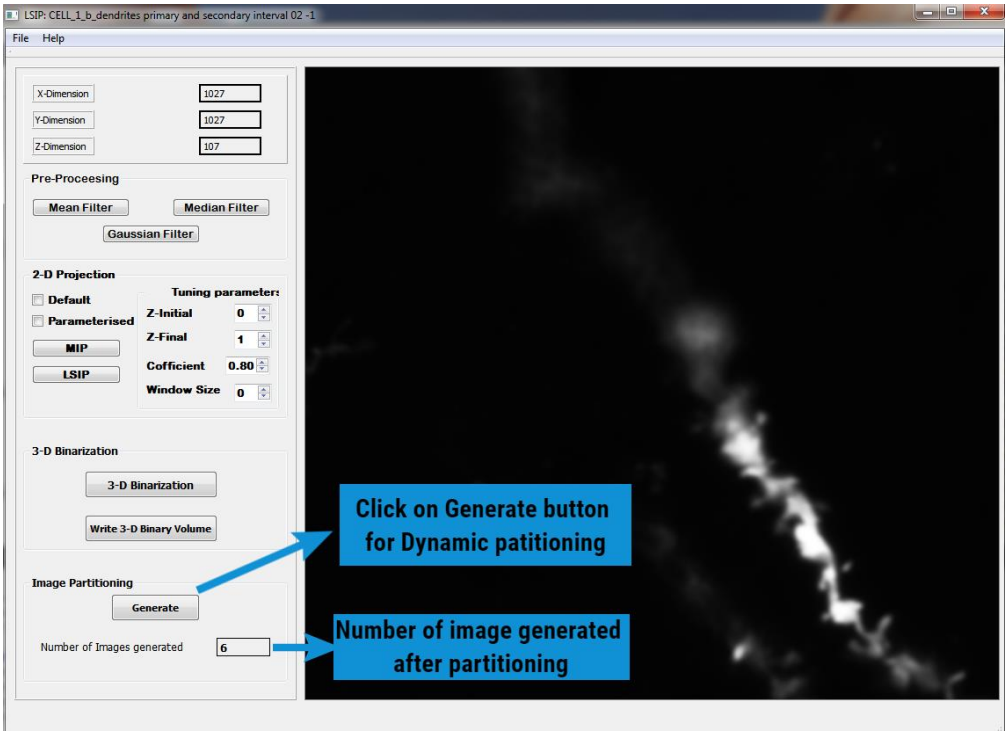

Figure 6-11 On Generate button clicked

Chapter 7

Conclusion

In this thesis a method is designed which is useful for pre-processing any neurological confocal microscopic images. Any further algorithm upon the 2D projection of 3D images is dependent on the pre-processing of the 3d image. The microscopic images are susceptible to noises and the focus of the microscope depends on the pinhole optimization. The high resolution structures are concentrated in the middle layer of the image stack. This makes the visualization of the image stack difficult.

This thesis acknowledges these problems and provides solutions for the same. Noise minimizing 3D filters is incorporated in this thesis. Those are essential to be applied in any biological images before further processing.

This thesis has proposed Locality sensitive intensity projection which gives better result in case of our dataset and likely to optimise the result in every case. It ensures that the result is not degraded from MIP image. This gives a significance improvement not only in terms of the pre-processing but also this projection will generate better result in 2D spine analysis algorithm.

This thesis also proposes a 3D adaptive local binarization technique which fundamentally uses the Locality sensitivity. 3D binarization is highly prone to noise and it is very important to categorise the background and foreground of those data. Our proposed algorithm generates results which preserves the actual structure of the spines in 3D volumes although they are concentrated at the middle layers of the stack.

The visualization of entwined complex neurological images and further processing of the whole stack is computationally challenging and also it generates misleading results in 2d projections. Our proposed method dynamically generates multiple 3d images from a single 3D image stack.
Nevertheless, this method has few limitations. The proposed Z-projection
Is not parameter-free, and to tune the parameters the users must have expertise in the subject. The proposed method is computationally challenging when the window size exceeds. These problems can be solved in future. The binarization result is not information preserving on the lower and upper slices of the stack. Advance studies can be done on this issue. Dynamic Image partitioning has given good result on synthetic data set but further scope of improvement for better time complexity can be done.

References

[1] F. Amyot *et al.*, "A Review of the Effectiveness of Neuroimaging Modalities for the Detection of Traumatic Brain Injury.," *J. Neurotrauma*, vol. 32, no. 22, pp. 1693–721, Nov. 2015.

[2] "How the spinal cord works - Reeve Foundation." [Online]. Available: https://www.christopherreeve.org/living-with-paralysis/health/how-the-spinal-cord-works. [Accessed: 15-May-2019].

[3] J. M. Mateos-Pérez, M. Dadar, M. Lacalle-Aurioles, Y. Iturria-Medina, Y. Zeighami, and A. C. Evans, "Structural neuroimaging as clinical predictor: a review of machine learning applications," Jun. 2018.

[4] C. J. Price and K. J. Friston, "Functional ontologies for cognition: The systematic definition of structure and function," *Cogn. Neuropsychol.*, vol. 22, no. 3–4, pp. 262–275, May 2005.

[5] R. Kamathe and K. Joshi, “NEUROIMAGING AND PATTERN RECOGNITION TECHNIQUES FOR AUTOMATIC DETECTION OF ALZHEIMER’S DISEASE: A REVIEW,” *ICTACT J. IMAGE VIDEO Process.*, p. 1, 2017.

[6] Z. Zhang, H. Huang, D. Shen, and Alzheimer’s Disease Neuroimaging Initiative, “Integrative analysis of multi-dimensional imaging genomics data for Alzheimer’s disease prediction,” *Front. Aging Neurosci.*, vol. 6, p. 260, Oct. 2014.

[7] F. Huss, “In vitro and in vivo studies of tissue engineering in reconstructive plastic surgery,” 2005.

[8] D. Semwogerere and E. R. Weeks, “Confocal Microscopy.”

[9] Y. Ozaki, “Application of Confocal Laser Scanning Microscopy (CLSM) for Observing Adhesives in Paper,” *J. Adhes. Sci. Technol.*, vol. 25, no. 6–7, pp. 723–741, Jan. 2011.

[10] B. R. Masters and P. T. C. So, “Confocal microscopy and multi-photon excitation microscopy of human skin in vivo,” 2001.

[11] J. N. Farahani, M. J. Schibler, and L. A. Bentolila, “Stimulated Emission Depletion (STED) Microscopy: from Theory to Practice.”

[12] Y. Waerzeggers, P. Monfared, T. Viel, A. Winkeler, and A. H. Jacobs, “Mouse models in neurological disorders: Applications of non-invasive imaging,” *Biochim. Biophys. Acta - Mol. Basis Dis.*, vol. 1802, no. 10, pp. 819–839, Oct. 2010.

[13] M. F. Lythgoe, N. R. Sibson, and N. G. Harris, “Neuroimaging of animal models of brain disease,” *Br. Med. Bull.*, vol. 65, no. 1, pp. 235–257, Mar. 2003.

[14] S. Matoug, A. Abdel-Dayem, K. Passi, W. Gross, and M. Alqarni, “Predicting Alzheimer’s disease by classifying 3D-Brain MRI images using SVM and other well-defined classifiers,” *J. Phys. Conf. Ser.*, vol. 341, no. 1, p. 012019, Feb. 2012.

[15] S. Basu *et al.*, “2dSpAn: semiautomated 2-d segmentation, classification and analysis of hippocampal dendritic spine plasticity,” *Bioinformatics*, vol. 32, no. 16, pp. 2490–2498, Aug. 2016.

[16] O. Wijardi, “Survey of 3d image segmentation methods,” *Keywords image Process. 3d image segmentation Bin.*, vol. 123, no. 123, p. Kaiserslautern, Germany, 2007.

[17] T. Walter *et al.*, “Visualization of image data from cells to organisms,” *Nat. Methods*, vol. 7, no. 3, pp. S26–S41, Mar. 2010.

[18] N. Kumar and M. Nachamai, “Noise Removal and Filtering Techniques used in Medical Images,” *Orient. J. Comput. Sci. Technol.*, vol. 10, no. 1, pp. 103–113, Mar. 2017.

[19] A. Kumar Boyat and B. Kumar Joshi, “Signal & Image Processing,” *An Int. J.*, vol. 6, no. 2, 2015.

[20] U. Sara and I. Journals, “Study on Different Image Quality Assessment Techniques for Gray Scale Images,” *IREJournals*.

[21] “Workshop 5 The normal distribution,” no. April 1810, 2016.

[22] I. Journal, E. M. Alleddawi, and Z. Alqadi, “Comparative Analysis of Methods Used to Remove Salt and Pepper Noise,” *IJCSMC*.

[23] A. Kaur and K. Singh, “SPECKLE NOISE REDUCTION BY USING WAVELETS.”

[24] “Gamma Distribution | Gamma Function | Properties | PDF.” [Online]. Available: https://www.probabilitycourse.com/chapter4/4_2_4_Gamma_distribution.php. [Accessed: 30-Apr-2019].

[25] N. K. Gill and A. Sharma, “Noise Models and De-noising Techniques in Digital Image Processing,” 2016.

[26] J. J. Gart, “The Poisson Distribution: The Theory and Application of Some Conditional Tests,” in *A Modern Course on Statistical Distributions in Scientific Work*, Dordrecht: Springer Netherlands, 1975, pp. 125–140.

[27] R. Tanikawa, T. Fujisawa, and M. Ikehara, “Image restoration based on weighted average of multiple blurred and noisy images,” in *2018 International Workshop on Advanced Image Technology (IWAIT)*, 2018, pp. 1–4.

[28] B. Goyal, A. Dogra, S. Agrawal, and B. S. Sohi, “Noise Issues Prevailing in Various Types of Medical Images,” *Biomed. Pharmacol. J.*, vol. 11, no. 3, pp. 1227–1237, Sep. 2018.

[29] O. Kayode Adedotun and O. M. Adegoke, “Noise Reduction Using Arithmetic Mean Filtering (A Comparison Study of Application to Different Noise Types),” *Int. J. Sci. Res.*, vol. 6, pp. 2319–7064, 2015.

[30] P. K. Garg, P. Verma, and A. Bhardwaz, “A Survey Paper on Various Median Filtering Techniques for Noise Removal from Digital Images,” *Am. Int. J. Res. Formal, Appl. Nat. Sci. AIJRFANS*, pp. 14–334, 2014.

[31] E. Elboher and M. Werman, “Efficient and Accurate Gaussian Image Filtering Using Running Sums.”

[32] S. Bruckner, “Performing Maximum Intensity Projection with the Visualization Toolkit,” *Semin. Pap. Austria*, no. February, 2002.

[33] F. Ling and L. Yang, “Improved on Maximum Intensity Projection,” in *2009 International Conference on Artificial Intelligence and Computational Intelligence*, 2009, pp. 491–495.

[34] D. Iwai, S. Mihara, and K. Sato, “Extended Depth-of-Field Projector by Fast Focal Sweep Projection,” *IEEE Trans. Vis. Comput. Graph.*, vol. 21, no. 4, pp. 462–470, Apr. 2015.

[35] Chenguang Ma, Jinli Suo, Qionghai Dai, R. Raskar, and G. Wetzstein, “High-rank coded aperture projection for extended depth of field,” in *IEEE International Conference on Computational Photography (ICCP)*, 2013, pp. 1–9.

[36] A. Shihavuddin *et al.*, “Smooth 2D manifold extraction from 3D image stack,” *Nat. Commun.*, vol. 8, no. May, pp. 1–8, 2017.

[37] P. A. Mahajan and S. A. Patil, “A Review of Image Binarization Techniques for Ancient Degraded Documents,” *Int. J. Sci. Res.*, vol. 4, no. 11, pp. 54–56, 2016.

[38] S. & I. P. : A. I. J. (SIPIJ) and G. Sethi, “A BINARIZATION TECHNIQUE FOR EXTRACTION OF DEVANAGARI TEXT FROM CAMERA BASED

IMAGES.” .

[39] S. T. Khandare and A. D. Isalkar, “International Journal of Computer Science and Mobile Computing A Survey Paper on Image Segmentation with Thresholding,” 2014.

[40] T. R. Singh, S. Roy, O. I. Singh, T. Sinam, and K. M. Singh, “A New Local Adaptive Thresholding Technique in Binarization,” vol. 8, no. 6, pp. 271–277, 2012.

[41] R. K. Chatterjee and A. Kar, “Signal & Image Processing,” *An Int. J.*, vol. 8, no. 4, 2017.

[42] K. Khurshid, I. Siddiqi, C. Faure, and N. Vincent, “Comparison of Niblack inspired binarization methods for ancient documents,” *Doc. Recognit. Retr. XVI*, vol. 7247, no. January, p. 72470U, 2008.

[43] K. Bhargavi and S. Jyothi, “A Survey on Threshold Based Segmentation Technique in Image Processing,” *Int. J. Innov. Res. Dev.*, vol. 3, no. 12, pp. 234–39, 2014.

[44] S. Bangare, A. Dubal, P. S. Bangare, and S. Patil, *Reviewing otsu’s method for image thresholding*, vol. 10. 2015.

[45] M. Nandy and M. Banerjee, “A Comparative Analysis of Application of Niblack and Sauvola Binarization to Retinal Vessel Segmentation,” in *2017 3rd International Conference on Computational Intelligence and Networks (CINE)*, 2017, pp. 105–109.

[46] Z. Hadjadj, A. Meziane, Y. Cherfa, M. Cheriet, and I. Setitra, “ISauvola: Improved Sauvola’s Algorithm for Document Image Binarization,” 2016, pp. 737–745.

[47] S. Roy, A. Dey, K. Chatterjee, and S. K. Bandyopadhyay, “Signal & Image Processing,” *An Int. J.*, vol. 3, no. 6, 2012.

[48] S. Basu *et al.*, “Quantitative 3-D morphometric analysis of individual dendritic spines,” *Sci. Rep.*, vol. 8, no. 1, pp. 1–13, 2018.

[49] Z. Neyaz, R. Phadke, V. Singh, and C. Godbole, “Three-dimensional visualization of intracranial tumors with cortical surface and vasculature from routine MR

sequences," *Neurol. India*, vol. 65, no. 2, p. 333, 2017.

[50] K. M. Woolfrey and D. P. Srivastava, "Control of Dendritic Spine Morphological and Functional Plasticity by Small GTPases.," *Neural Plast.*, vol. 2016, p. 3025948, 2016.

[51] "Qt | Cross-platform software development for embedded & desktop." [Online]. Available: https://www.qt.io/. [Accessed: 15-May-2019].